Eur. Phys. J. A **30**, 357–367 (2006)
DOI 10.1140/epja/i2006-10129-2

THE EUROPEAN PHYSICAL JOURNAL A

Evolution of 2^+_γ wave functions and gamma-stiffness in well-deformed rare-earth nuclei

Ch. Hinke[1], R. Krücken[1,a], R.F Casten[2], V. Werner[2], and N.V. Zamfir[3]

[1] Physik Department E12, Technische Universität München, D-85748 Garching, Germany
[2] A.W. Wright Nuclear Structure Laboratory, Yale University, New Haven, CT 06520, USA
[3] National Institute of Physics and Nuclear Engineering, Bucharest-Magurele, Romania

Received: 9 May 2006 / Revised: 22 August 2006 /
Published online: 10 November 2006 – © Società Italiana di Fisica / Springer-Verlag 2006
Communicated by D. Schwalm

Abstract. The evolution of the structure of the gamma-vibrational band head 2^+_γ in well-deformed rare-earth nuclei is studied within the framework of RPA calculations using a quasiboson approximation based on the Nilsson model. The obtained evolution of the quasiparticle structure of the gamma-vibrational band head is shown to correlate well with the evolution of the same nuclei within the IBA symmetry triangle when described in the extended consistent-Q formalism. An empirical relation is presented that links the IBA parameter χ with the quasiparticle structure of the gamma-vibrational band head.

PACS. 21.10.Re Collective levels – 27.60.+j $90 \leq A \leq 149$ – 21.60.Jz Hartree-Fock and random-phase approximations – 21.60.Fw Models based on group theory

1 Introduction

The Nilsson deformed shell model [1] has been the benchmark for the understanding of the single-particle structure in well-deformed nuclei. In particular, the Nilsson model has been the basis for the study of the response of the nuclear many-body system to rotations. On the other hand, the evolution of collective degrees of freedom has been extensively studied with calculations in the framework of the interacting boson approximation (IBA) [2].

Recently, the extended consistent-Q formalism (ECQF) of the IBA [3] was used to map the structural evolution of deformed rare-earth Gd, Dy, Er, Yb, and Hf isotopes [4] within the IBA symmetry triangle [5]. It was found that towards mid-shell the Gd, Dy, and Er isotopes, while being well-deformed rotors, show a tendency of being less gamma-rigid, while the Yb and Hf isotopes become more gamma-rigid towards mid-shell. This work was followed by similar studies for the transitional W, Pt, and Os isotopes [6,7].

It is the purpose of this paper to provide some insight into the particular features of those IBA trajectories for the well-deformed rare-earth nuclei. We will show that for these nuclei the different structural evolution can be understood on the basis of some basic features *of the quasiparticle structure of the gamma-vibrational band*.

[a] e-mail: Reiner.Kruecken@ph.tum.de

The two-quasiparticle structure of the γ-vibrational 2^+_γ state for well-deformed stable even-even rare-earth nuclei has previously been calculated by Bès *et al.* [8] on the basis of a quasiboson approximation using quasiparticles constructed from single-particle energies and wave functions from the Nilsson model. The quasiparticle Hamiltonian for the description of the 2^+_γ state contained the $|K| = 2$ quadrupole interaction as well as the Coriolis interaction, which has been shown to be most important for an accurate description of transition probabilities.

Another well-known approach for the description of low-lying non-rotational states in strongly deformed even-even nuclei in the rare-earth region has been the quasiparticle-phonon model by Soloviev [9–11]. The model was applied to ^{156,158,160}Gd, ^{160,162,164}Dy, ^{166,168}Er [12], as well as ^{172}Yb [13]. In these calculations it was shown that the 2^+_γ state in all these nuclei is to more than 90% a one-phonon excitation of multipole order $\lambda\mu = 22$. The most significant two-quasiparticle components have been listed in refs. [12,13].

Since those previous studies have not been carried out for all the nuclei investigated within the IBA study of ref. [4], we have performed a systematic investigation based on the concept used in ref. [8], a simple RPA approach on the basis of a quasiboson approximation. Since we are only interested in the evolution of the major two-quasiparticle components in the wave functions of the 2^+_γ states that are related to the gamma degree of freedom,

we will neglect Coriolis mixing as well as other interaction components that were taken into account in refs. [8,12,13]. While our results will therefore certainly not provide the best description of the detailed single-particle structure of these nuclei, they will nevertheless allow us to reproduce main features that are relevant to understand the structural evolution with respect to the gamma-softness observed in the IBA study of ref. [4].

The paper is organized in the following way. We first briefly review the basic ingredients of the quasiboson model that is based on the formalism of the random-phase approximation. Thereafter, the resulting quasiparticle components of the wave function of the 2^+_γ states in the nuclei of interest are discussed and compared to previous calculations. In a next step, the distributions of two-quasiparticle components are quantified allowing to distinguish if a gamma-vibrational state contains only few major or many small two-quasiparticle components, respectively. Afterwards, an overview of the previous IBA results and their relation to the stiffness of the collective potential in gamma-direction is given. The results for the quasiparticle distributions and the IBA results motivate the definition of a single new quantity, the gamma structure function. We will provide arguments that this quantity should be related to the stiffness of the collective potential in the gamma-direction and that it shows a qualitative correlation with the IBA results. In a final step we introduce an empirical analytic relation that connects this gamma structure function with the position of a specific nucleus in the symmetry triangle of the IBA.

2 The model

We use a simple calculation based on the formalism of the random-phase approximation (RPA) (see, *e.g.* [14]) in which we assume that the wave function of the γ-vibrational 2^+_γ state is made up completely of coherent two-quasiparticle excitations from the ground state by means of the $Q_{2\pm2} = r^2 Y_{2\pm2}$ operator.

The $Q_{2\pm2}$ operator connects Nilsson single-particle states $K^\pi[Nn_z\Lambda]$, with $K = \Lambda+\Sigma = \Lambda\pm1/2$ that obey the selection rule $\Delta N = 0, \pm2$, $\Delta n_z = 0$, $\Delta\Sigma = 0$, $\Delta K = \pm2$, $\Delta\Lambda = \pm2$, and $\Delta\pi = +1$, where N is the principal quantum number denoting the major shell, n_z the number of nodes in the z-direction (along the symmetry axis of the deformed potential), Λ the component of the orbital angular momentum along the z-axis, and Σ the projection of the intrinsic nucleon spin onto the z-axis.

Within the straightforward RPA approach incorporating the quasiboson approximation we determine the so-called forward and backward amplitudes x_{mi} and y_{mi}, respectively, of those Nilsson states m and i which are connected by the selection rules of the quadrupole operator and which are making up the collective wave function

$$|c\rangle = \sum_{mi} \left(x_{mi} a^\dagger_m a^\dagger_i |0\rangle - y_{mi} a_m a_i |0\rangle \right). \qquad (1)$$

The value of the square of the forward amplitude minus the square of the backward amplitude considered separately for each contributing orbital combination is an indicator for the relevance of those states in the wave function. Of course the sum over all these values is normalized to one, *i.e.*

$$\sum_{mi} C_{mi} = \sum_{mi} \left(|x_{mi}|^2 - |y_{mi}|^2 \right) = 1. \qquad (2)$$

The matrix elements between the relevant states have been evaluated using the analytically determined wave functions which are solutions to the anisotropic three-dimensional harmonic-oscillator potential [15]. In the limit of large deformations these solutions are exactly valid. In dealing with medium deformed nuclei with $\beta \approx 0.3$ linear combinations of these wave functions have to be considered. However, one component of the linear combination is always much larger than any of the rest indicating an almost pure state. In the present calculation it is therefore a reasonable approximation to work with the exact solutions for large deformations.

The pairing residual interaction is included both by modifying the interaction matrix elements with the well-known BCS emptiness and fullness factors (U_i, V_i) and by transforming the Nilsson single-particle energies to quasiparticle energy levels. The generalized Fermi energy used in the BCS theory is approximated by the Fermi energy determined by the highest occupied level in the Nilsson model neglecting pairing correlations. The pairing gaps are extracted from the experimental one-nucleon separation energies of adjacent nuclei.

The model was applied to the well-deformed rare-earth nuclei with $R_{4/2} = E(4^+_1)/E(2^+_1) > 2.9$. This selection includes the nuclei near the phase/shape transition ^{152}Sm, ^{154}Gd, ^{156}Dy, and ^{162}Yb, where the results should be taken with some caution, in particular, since large fluctuations in the deformation parameter β are to be expected, making the assignment of the two-quasiparticle structure of the involved states less reliable. Nevertheless, the results for these nuclei are helpful in following the trends for the isotopic chains.

In order to determine the relevant quasiparticle contributions we evaluated the Nilsson single-particle energies at the experimentally known quadrupole deformation parameters [16] and use the tabulated values for the one-nucleon separation energies [17] for the determination of the pairing energies.

It should be emphasized that the well-deformed rare-earth nuclei, which we considered in this work, are without exception in good approximation axially symmetric in their ground states [18] and the minimum of the total energy surface is located at $\gamma = 0°$. For the description of the properties of these well-deformed nuclei it is therefore a good approximation to consider only axially symmetric shapes [19]. Thus, in order to determine the energies and wave functions of the single-particle states upon which the gamma-vibration is built, we only considered the experimentally known quadrupole deformation parameter β for the ground state of each nucleus [16] and fixed the asymmetry parameter γ at a value of zero. This procedure was also applied by Bès *et al.* [8] in their work and in

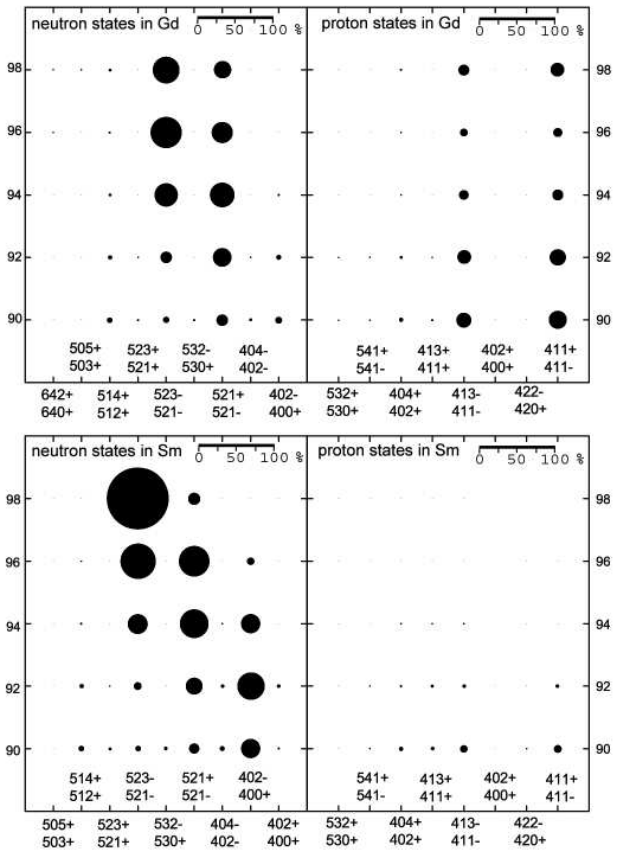

Fig. 1. Most relevant squared amplitudes of two-quasiparticle states contributing to the 2^+_γ state in the well-deformed even-even Sm and Gd isotopes. The diameter of the circles represents the probability with which each two-quasiparticle state contributes to the total wave function. A scale is plotted to make it possible to estimate the total contribution of the state to the wave function in percent.

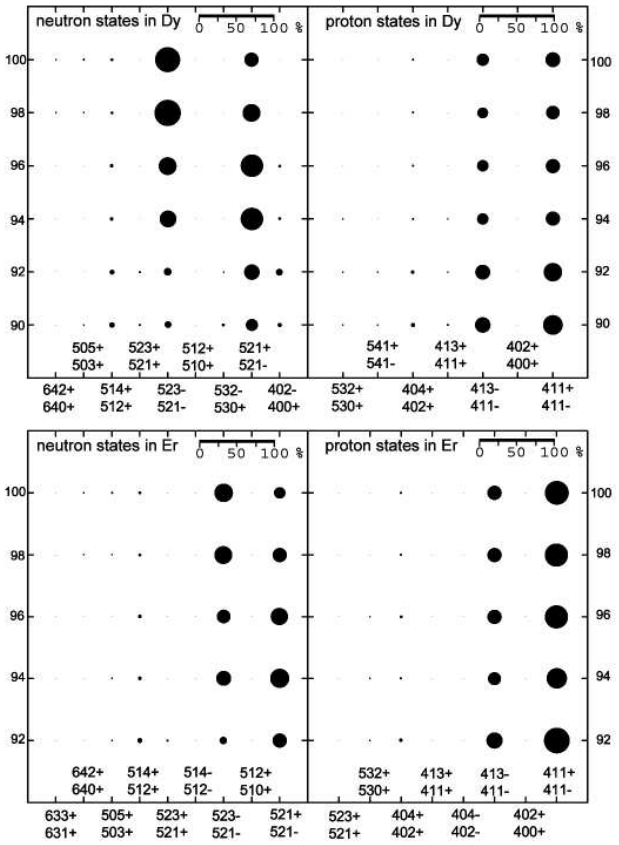

Fig. 2. Same as fig. 1 for Dy and Er isotopes.

the quasiparticle-phonon model by Soloviev [9–11] only an axisymmetric potential is considered for the calculation of vibrational states.

Of course the potential is not infinitely steep and zero-point motion leads to a finite but small $\gamma_{eff} \approx 0°$–$10°$, which depends on the stiffness of the potential leading to highly excited 2^+_γ states for a very stiff potential and lower excitation energy for less stiffness. It should be pointed out that all nuclei under consideration show rather gamma-rigid potentials, however with some variation in the stiffness. It is exactly this variation of the stiffness that our results will relate to.

The well-known RPA equations (see, *e.g.* [14]) lead to a dispersion relation. This relation contains all relevant information about the structure (quasiparticle energies, matrix elements) of the nucleus. The usual way to obtain the collective wave function is to determine the energy eigenvalues from this dispersion relation and then use the lowest solution as input to calculate the forward and backward amplitudes. However, the value (strength) of the coupling constant of the quadrupole interaction, which is necessary to fix the solution, cannot be derived from theory. In the paper by Bès *et al.* [8] an average fit value for the coupling constant was chosen to reasonably reproduce experimental excitation energies of the 2^+_γ states in the rare-earth region. Hernández *et al.* [20] considered in their approach for each nucleus a different coupling constant in order to exactly reproduce the experimental energy when they calculated reduced transition probabilities. This latter procedure is equivalent to using the experimental excitation energies of the 2^+_γ states directly to determine the amplitudes, resulting in a rather small variation of the coupling constant among the rare-earth nuclei under consideration. Since the experimental energy of the 2^+_γ state is unknown for ^{158,160}Sm we have used the coupling constant obtained for ^{156}Sm in order to calculate the energy and composition of their 2^+_γ states.

Finally, we obtain the following relation for the squares of the amplitudes $C^{\pi,\nu}_{mi}$ (π and ν denote the proton and neutron contributions, respectively) of the two-quasiparticle states m, i in the wave function of the γ-vibration:

$$C^{\pi,\nu}_{mi} \propto \left|\langle m|r^2 Y_{2\pm 2}|i\rangle\right|^2 \cdot (U_m V_i + U_i V_m)^2 \cdot \left[(E_\gamma - (E_m + E_i))^{-2} - (E_\gamma + (E_m + E_i))^{-2}\right]. \quad (3)$$

Due to the fact that we neglect Coriolis and other interaction components [8,12] the calculated electromagnetic

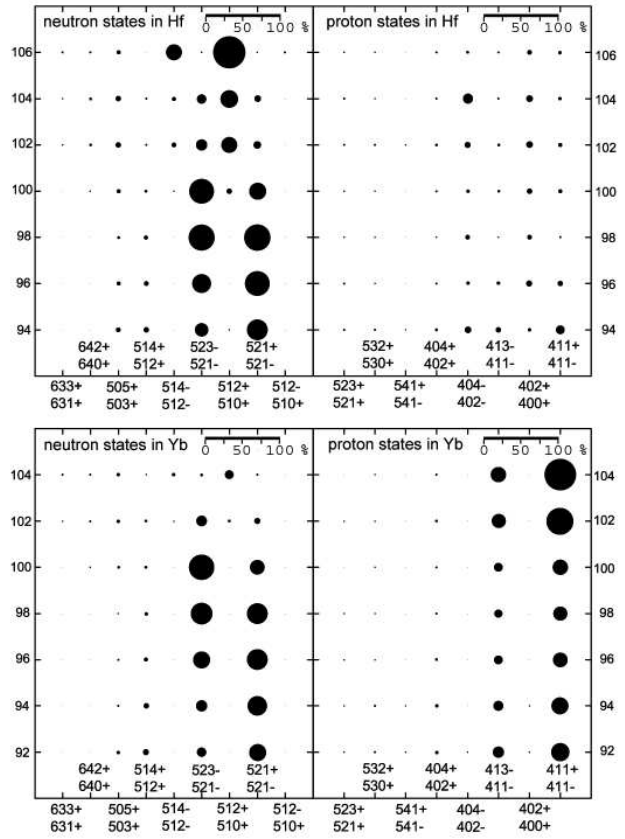

Fig. 3. Same as fig. 1 for Yb and Hf isotopes.

transition matrix elements (not presented here) do not reproduce the experimental trends. The $E2$ matrix element is very sensitive to the many small components of the wave function, which depend on those extra interaction terms. However, the order of magnitude of the $E2$ matrix elements is reproduced in our calculations, indeed showing the collective character of the 2^+_γ states.

3 Results

3.1 Major components of the wave function

Figures 1-3 show the most relevant wave function components contributing to the 2^+_γ wave function in the well-deformed Sm, Dy, Gd, Er, Yb, and Hf isotopes. The diameter of the circles indicates the probabilty of each two-quasiparticle wave function component with respect to the total wave function. We assume here that the wave function of the 2^+_γ state is completely described by those wave function components. This rather crude assumption seems to be justified when comparing our results to those by Bès *et al.* [8], which are shown in fig. 4 for ^{156,158,160}Gd and in fig. 5 for ^{160,162,164}Dy. For those nuclei also calculations by Soloviev *et al.* [12] have been performed, which are also shown in the figures for comparison. Overall, one can see reasonable agreement with both previous calculations, although the admixture of two-quasiparticle states

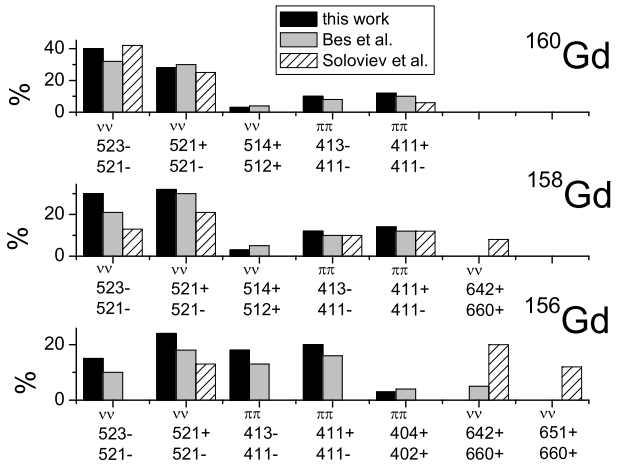

Fig. 4. Comparison of the strongest two-quasiparticle components in the wave function of the 2^+_γ state (in percent) in ^{156,158,160}Gd in the calculations from this work with those by Bès *et al.* [8] and by Soloviev *et al.* [12].

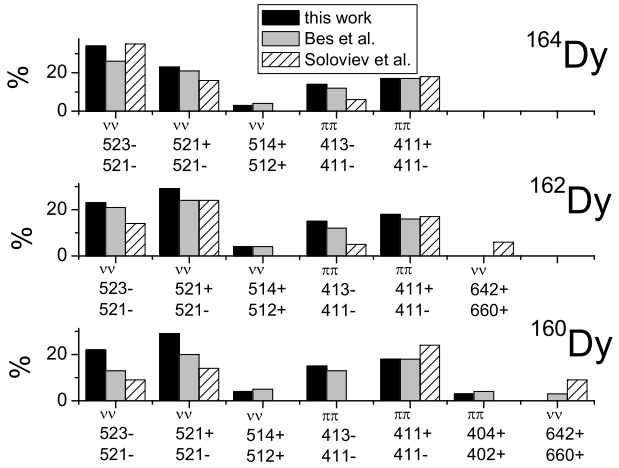

Fig. 5. Comparison of the strongest two-quasiparticle components in the wave function of the 2^+_γ state (in percent) in ^{160,162,164}Dy in the calculations from this work with those by Bès *et al.* [8] and by Soloviev *et al.* [12].

that cannot be connected by the Y_{22} operator is in some cases significant, in particular in the calculation for ^{156}Gd by Soloviev *et al.* [12]. However, the agreement seems sufficiently good to give confidence to our schematic calculation, that primarily aims to investigate the trends in the contributions of those two-quasiparticle states that can be connected by the Y_{22} operator and therefore should provide information on trends in the gamma-rigidity of these nuclei.

It is apparent in figs. 1-5 that in most cases only a few quasiparticle configurations for protons and neutrons dominate the wave function of the 2^+_γ state. This is observed not only in our calculations but also in those performed by Bès *et al.* [8] and Soloviev *et al.* [12]. These long known results seem to be contradicting the notion

of the 2^+_γ state being a collective excitation. Nevertheless, the calculations are in general agreement with the results of experimental investigations (see, *e.g.* [13]). At the same time the experimental $B(E2)$-values for the transition from the 2^+_γ to the ground state show collective character. In this context it has to be repeated that also the smaller quasiparticle contributions, which all add up coherently, do play an important role for the collectivity of the transition strength. At the same time the calculations consistently show that the gamma-vibrational state always carries several dominant quasiparticle components.

3.2 The distribution functions S_ν, S_π

We now want to use the obtained results to evaluate and quantify the distribution of different two-quasiparticle contributions to the wave function of the γ-vibrational 2^+_γ states of the nuclei under consideration. These results will in turn be used for a comparison to the structural evolution of these deformed nuclei within the symmetry triangle of the IBA [4,6,7].

We take into account all squared amplitudes C_{mi} that are larger than 0.001 and label them as $C^{\pi,\nu}_{(h)}$ for protons and neutrons, respectively, in arbitrary order with integer numbers $h = 1, 2, \ldots, j$, where j is the number of two–quasi-proton/neutron states contributing to the 2^+_γ states with squared amplitudes above the cut-off value. Therefore we construct a distribution function $S_\nu(j)$ for the neutrons in the following way:

$$S_\nu(j) = \frac{\sum_{h=1}^{j}\sum_{l=1}^{j}|C^\nu_{(h)} - C^\nu_{(l)}|}{2\cdot(j-1)\cdot\left(\sum_{h=1}^{j} C^\nu_{(h)}\right)}. \qquad (4)$$

In the same way we construct a distribution function $S_\pi(k)$ for the k proton contributions above the cut-off limit,

$$S_\pi(k) = \frac{\sum_{h=1}^{k}\sum_{l=1}^{k}|C^\pi_{(h)} - C^\pi_{(l)}|}{2\cdot(k-1)\cdot\left(\sum_{h=1}^{k} C^\pi_{(h)}\right)}. \qquad (5)$$

As one can easily verify, the distribution functions $S_{\eta=\nu,\pi}$ can have values between 0 and 1. For the case that exactly one two-quasiparticle excitation contributes to the 2^+_γ wave function one obtains $S_\eta(j) = 1$, while $S_\eta(j) = 0$ is reached in the case that all j two-quasiparticle excitations contribute exactly with the same squared amplitudes.

In the forthcoming discussion we want to compare the distribution functions for different nuclei for which the numbers of squared amplitudes above the cut-off value may be different. Therefore a straightforward normalization to the number of relevant wave function components has been applied. From now on we will call these normalized distribution functions S_π and S_ν, respectively.

Besides the distribution functions S_π and S_ν we can, within the framework of our model, also determine the fractions $f_\pi = \sum C^\pi_{(h)}$ and $f_\nu = \sum C^\nu_{(h)}$ of the contribution of proton and neutron quasiparticles to the wave function of the 2^+_γ state.

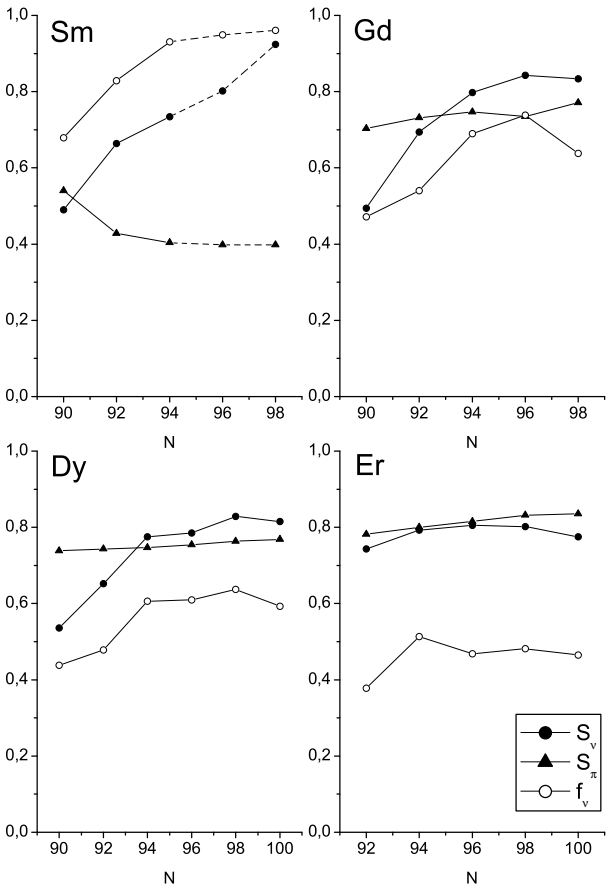

Fig. 6. Distribution functions S_ν and S_π for neutrons and protons, respectively, as a function of neutron number for well-deformed even-even Sm (top left), Gd (top right), Dy (bottom right), and Er (bottom left) isotopes together with the fraction f_ν of neutrons in the wave function of the 2^+_γ state (see text for details). For ^{158,160}Sm we have used the same quadrupole coupling strength as in ^{156}Sm in order to determine the energy of the 2^+_γ state. Therefore the results are indicated by dashed lines.

Figures 6-7 show the distribution functions S_π, S_ν, as well as the fraction f_ν for well-deformed Sm, Dy, Gd, Er, Yb, and Hf isotopes.

One can observe some general features for the distribution functions. The proton distribution function S_π remains almost constant as a function of neutron number for most elements. Exceptions to this behavior occur only, *e.g.* in ^{174}Hf, due to a variation of the quadrupole deformation causing variations in the occupation of quasiparticle states. For the neutron distribution function S_ν there are significant variations as a function of neutron number due to changes of the Fermi energy as one moves along an isotopic chain. Therefore, the development of the neutron distribution function S_ν is of prime interest.

Another remarkable feature is the strong correlation in most nuclei between S_ν and f_ν, the fraction of the entire collective wave function carried by all the neutron states together. To avoid any misunderstandings it should be

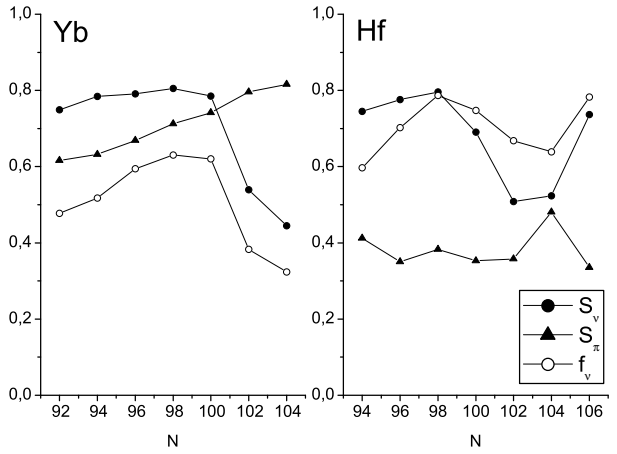

Fig. 7. Same as fig. 6 for Yb (left) and Hf (right) isotopes.

re-emphasized that S_ν only takes the distribution among the neutron states into account. Due to its construction it is completely independent of the neutron fraction of the wave function. However, the evaluated data shows that the process of building up a few dominant neutron basis states when moving along the isotopic chain is most often connected with the transfer of importance in the entire wave function from the proton states to the neutron states.

In the subsequent discussion we will elaborate on the evolution of the distribution functions S_π and S_ν and the fractions f_ν and f_π along the different isotopic chains. We will also qualitatively relate this behavior to the position of the individual nuclei within the symmetry triangle of the IBA.

4 Discussion

In this section we will discuss how the results of our model calculations relate to the stiffness of a collective potential (characterized by the quadrupole deformation β and the asymmetry parameter γ) in the direction of gamma. Before we discuss the evolution of the above results along the various isotopic chains, it is necessary to recall the results of the IBA fits of ref. [4]. We will use the IBA results as an indicator of the gamma-stiffness and therefore will first introduce this connection. After discussing the IBA results we will introduce a new quantity for a quantitative comparison of microscopic and IBA results. Finally, we will present an empirical relation that connects our results analytically to the IBA parameters.

4.1 Summary of IBA results

The IBA calculations in ref. [4] show quite different trajectories for Dy, Gd, Er on one side and Yb, Hf on the other side (see fig. 14 of ref. [4]) within the IBA symmetry triangle. The calculations are based on the ECQF formalism where the simplified IBA Hamiltonian only consists of the

Table 1. Angle $\theta = (180^\circ/\pi) \cdot (\pi/3 + (2/\sqrt{7})\chi(\pi/3))$ in degrees within the IBA symmetry triangle for the well-deformed Gd, Dy, Er, Yb, and Hf from ref. [4] as a function of neutron number.

N	θ (Gd)	θ (Dy)	θ (Er)	θ (Yb)	θ (Hf)
90	10.1	21.5			
92	21.0	29.6	32.8	41.0	39.6
94	23.7	37.8	36.0	36.4	36.0
96	36.0	45.9	43.2	33.7	32.8
98	46.4	48.2	45.9	32.3	24.2
100			43.7	28.7[a]	21.9
102				19.6[a]	10.1
104					16.5

[a] Parameter χ obtained by considering the second excited 0^+ state as the first excited collective 0^+ state [4].

d-boson number operator and the quadrupole operator,

$$H = c \cdot \left[(1-\zeta)\hat{n}_d + \frac{\zeta}{4N_B}\hat{Q}\cdot\hat{Q}\right] = \epsilon_d \hat{n}_d + \kappa \hat{Q}\cdot\hat{Q}\,. \quad (6)$$

Here N_B is the total IBA boson number of the nucleus. ϵ_d and κ are related to ζ and the scaling factor c by $\epsilon_d = c\cdot(1-\zeta)$ and $\kappa = (c\cdot\zeta)/(4N_B)$, respectively.

Here we want to concentrate on the behavior of the polar angle θ defined as [4]

$$\theta = \frac{\pi}{3} + \frac{2}{\sqrt{7}}\chi\frac{\pi}{3}. \quad (7)$$

Table 1 summarizes the angles θ resulting from the IBA fits in ref. [4].

In order to obtain more direct information on the gamma-rigidity it is instructive to consider the potential energy surface in the classical limit of the intrinsic state formalism [21,22]. The expectation value for the Hamilton operator is given by

$$\langle\hat{H}\rangle = \epsilon_d\langle\hat{n}_d\rangle + \kappa\langle\hat{Q}\cdot\hat{Q}\rangle \quad (8)$$

with [23]

$$\langle\hat{n}_d\rangle = \frac{N_B\beta^2}{1+\beta^2} \quad (9)$$

and

$$\langle\hat{Q}\cdot\hat{Q}\rangle = \frac{N_B}{1+\beta^2}\left(5+(1+\chi^2)\beta^2\right) + \frac{N_B(N_B-1)}{(1+\beta^2)^2}\left(\frac{2}{7}\chi^2\beta^4 - 4\sqrt{\frac{2}{7}}\chi\beta^3\cos(3\gamma) + 4\beta^2\right). \quad (10)$$

The stiffness K of the potential $V(\beta,\gamma) \equiv \langle H\rangle$ in the γ-direction at its minimum value $V(\beta_{min},\gamma_{min})$ is defined as

$$K \equiv \frac{\partial^2 V(\beta,\gamma)}{\partial\gamma^2}|_{\beta_{min},\gamma_{min}}.$$

This yields the following expression which is proportional to the stiffness:

$$K = 36\sqrt{\frac{2}{7}} \cdot \kappa \cdot \frac{N_B(N_B-1)}{(1+\beta^2_{min})^2} \cdot \chi \cdot \beta^3_{min}. \qquad (11)$$

It was already mentioned that the well-deformed nuclei which were considered here are axially symmetric in their ground states and the minimum of the potential energy surface is always located at $\gamma_{min} = 0°$, which is also the only possibility within the IBA-1.

The stiffness K is directly proportional to the IBA parameter χ, which in turn determines the polar angle θ. However, K also depends on the strength κ of the quadrupole-quadrupole interaction, the boson number N_B, and the equilibrium deformation β_{min}. This means that large values of χ alone are not sufficient for gamma-rigidity.

For given κ/ϵ_d or ζ values a value of $\theta = 0°$ ($\chi = -1.32$) corresponds to a large gamma-stiffness while $\theta = 60°$ ($\chi = 0$) corresponds to completely gamma-soft nuclei. However, the scale is highly non-linear since also nuclei with $\theta = 50°$ can still be good axial symmetric rotors with large but somewhat reduced gamma-stiffness. It is worthwhile pointing out that an equivalent discussion of the potential would in principle also be possible within the geometric collective model (GCM) [24–26], for which an analogous structural triangle can be defined [27]. Seven-parameter GCM fits to some of the Gd, Dy, Er, and Yb isotopes under consideration here also describe the nuclei as axially symmetric [28].

Let us now turn to the evolution of the angle θ along the different isotopic chains [4]. After the phase transition from spherical to deformed shapes in the IBA symmetry triangle, which occurs at neutron numbers around 90–92 for the nuclei under consideration, the Gd, Dy, and Er isotopes tend with growing neutron number towards large angles θ in the triangle into the direction of $O(6)$ ($\theta = 60°$). At the same time the values of ζ increase monotonically for those elements. On the other hand, the Yb and Hf isotopes approach with increasing neutron number the $U(5)$-$SU(3)$ leg of the triangle ($\theta = 0°$) with almost constant values of ζ around 0.6–0.7.

Results obtained using eq. (11) show that the neutron-rich Gd, Dy, and Er isotopes (with large θ angles) have a less stiff potential with respect to γ than the most neutron-rich Yb and Hf nuclei. Nevertheless, the neutron-rich Gd and Dy isotopes are still good axially symmetric rotors with $R_{4/2} = E(4^+_1)/E(2^+_1) > 3.0$ although they are close to the $O(6)$ corner of the triangle with angles θ of about 50°. Therefore, it is important to point out that the stiffness of the potential in γ-direction stays large for all well-deformed rare-earth nuclei and consequently it would be wrong to label the neutron-rich Gd and Dy nuclei as gamma-soft in the sense of the $O(6)$ nuclei like, *e.g.*, ^{196}Pt [29].

4.2 Definition of a gamma structure function

Now that we have some idea of the structure of the nuclei of interest in terms of the gamma-stiffness of the collective potential, we want to relate this information to the results of our RPA calculations. Therefore, we define a new quantity that combines the information contained in the values of the distribution functions $S_{\pi,\nu}$ and the proton and neutron fractions $f_{\pi,\nu}$. For this we introduce the *gamma structure function*

$$\Gamma = 4 \cdot [f_\pi \cdot f_\nu \cdot S_\pi \cdot S_\nu] \qquad (12)$$

that can take on values between 0 and 1.

Figure 8 shows the gamma structure function Γ as a function of the neutron number for the well-deformed Sm, Dy, Gd, Er, Yb, and Hf isotopes.

Before we discuss the behavior of Γ for the different nuclei in the next subsection we would like to motivate the reason we expect this quantity indeed to correlate to the gamma-stiffness.

We assume that in the gamma-vibrational state protons and neutrons oscillate coherently in phase with each other. It is reasonable to suppose that in nuclei where protons and neutrons contribute with more or less equal fractions to the wave function, such oscillations are relatively easy to achieve. In other words, they are at lower energies as compared to nuclei where the wave function is dominated by one type of nucleons. In the latter case the oscillation of the one type of nucleons is strongly damped through the strong proton-neutron interaction with the non-participating nucleon type. The excitation of such a mode would cost more energy and thus the collective potential be more stiff as compared to an equal contribution of protons and neutrons. This argument motivates that a quantity to describe the gamma-stiffness should include the product of f_ν and f_π, which is maximal for $f_\nu = f_\pi$, indicating a less stiff potential.

In order to motivate the second ingredient of Γ we need to look back at the IBA results above. The neutron-rich

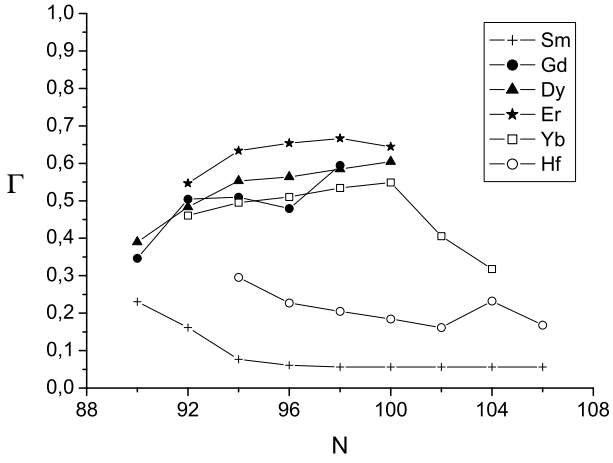

Fig. 8. Gamma structure function Γ as a function of neutron number for well-deformed Sm, Gd, Dy, Er, Yb, and Hf isotopes.

Gd, Dy, and Er nuclei have a relatively small gamma-rigidity (large θ) and exhibit large values of both S_π and S_ν. For nuclei with large gamma-rigidity (small θ) either both distribution functions are rather small, *e.g.* $^{174}_{72}\mathrm{Hf}_{102}$, or there exists a large imbalance between the two distribution functions, *e.g.* $^{174}_{70}\mathrm{Yb}_{104}$ and $^{156}_{62}\mathrm{Sm}_{94}$. Guided by this behavior the gamma structure function should contain the product $S_\pi \cdot S_\nu$. As a result, large values for Γ, which should relate to a less stiff gamma-potential, are obtained if the wave functions for protons and neutrons both contain a few strongly contributing quasiparticle states.

It is important to point out that throughout our calculations (excluding Sm in which the proton fraction f_π of the wave function drops dramatically for higher neutron numbers) the wave functions are never dominated by only one two-quasiparticle state for protons or neutrons. In order to produce a collective state it seems to be necessary to have at least a few dominant orbital combinations in the wave function (typically two for protons and two for neutrons). Therefore, the extreme case in which the distribution function S_ν and S_π are equal to one (and $\Gamma \approx 1$) does not occur in reality.

The definition of Γ thus leads to large values (≈ 0.6) if only a few neutron and proton states contribute to the wave function with equal strength. This situation should correspond to a reduced gamma-stiffness. On the other hand, small Γ-values should correspond to the largest gamma-rigidity and are the result of an imbalance between protons and neutrons in the wave function or of an equal and small contribution of many quasiparticle states to the collective wave function. It is interesting to note that one obtains also a rather large value of $\Gamma \approx 0.5$ for the gamma-soft nucleus ^{196}Pt, consistent with our expectations despite the fact that the validity of our approximations is somewhat limited for transitional nuclei, such as W, Os, and Pt isotopes.

4.3 Evolution along isotopic chains

Above we have outlined the ingredients and results of our own calculations as well as the IBA fits. We now want to relate the structural evolution of well-deformed rare-earth nuclei within the IBA symmetry triangle, which depends partly on the gamma-stiffness of the potential, to the underlying single-particle structure of the gamma-vibrational state, which should microscopically be governing this stiffness. As pointed out above, the angle θ in the IBA symmetry triangle is directly related to the stiffness K of the potential in γ-direction. At the same time the gamma structure function Γ serves as a tool to reasonably distinguish and characterize various compositions of the microscopic wave functions of the gamma-vibrational state in a quantitative way. The stiffness of a collective potential should be clearly related to this microscopic structure.

In the succeeding subsections we show in detail for the isotopic chains of the different elements that there is a qualitative correlation between the gamma structure function Γ and the angle θ in the IBA symmetry triangle.

4.4 Sm isotopes

The Sm isotopes were not included in the aforementioned IBA study of ref. [4]. However, IBA calculations using a simplified Hamiltonian were performed for those nuclei by Scholten *et al.* [30]. In these calculations best fits for the even-even Sm isotopes with $N \geq 90$ were obtained using a value of $\chi = -\sqrt{7}/2$, placing those nuclei on the $U(5)$-$SU(3)$ leg of the symmetry triangle with $\theta = 0$. Thus, the Sm isotopes are the most gamma-rigid well-deformed nuclei considered in this study.

The distribution of the wave function among the neutron basis states in Sm (see fig. 1) changes its structure from an equal distribution of the wave function among many basis states to a dominance of few basis states leading to an increasing neutron distribution function S_ν in fig. 6.

Overall, the protons show a very low proton distribution function S_π. At the same time one can observe a complete dominance of the neutrons in the wave function of the 2^+_γ state with $f_\nu > 0.9$ for neutron numbers above $N = 92$. This fact should be reflected in experimental g-factors and electromagnetic reduced transition probabilities, potentially leading to strong $M1$ transitions from the 2^+_γ state to the 2^+_1 state. Indeed the extreme dominance of the neutrons is mainly responsible for the gamma-rigidity of the Sm isotopes and determines the low values of the gamma structure function Γ in fig. 8.

4.5 Dy, Gd, and Er isotopes

Within the IBA study of ref. [4] the Dy and Gd isotopes evolve with increasing neutron number from intermediate angles around 20–30° for $N = 92$, after crossing the transition from spherical to deformed phase, to larger angles close to 50° for $N = 98$. At the same time the radial coordinate increases so that the $O(6)$-$SU(3)$ leg of the symmetry triangle is reached near to the $O(6)$ corner of the triangle. Thus, these Dy and Gd nuclei show a reduced gamma-rigidity with increasing neutron number. Again, one should keep in mind that these nuclei have a rotational $R_{4/2}$-value and thus are still quite far from a gamma-soft potential.

After the phase transition from spherical to deformed ($N > 90$) the Gd and Dy isotopes show the same structural evolution. The proton distribution function S_π in fig. 6 stays on a relatively high level of about 0.7 for all isotopes, indicating that the quasiproton wave function is spread over only a few important basis states. Moving along the isotopic chain to higher neutron numbers the development among the neutron states changes their structure in Gd and Dy from an equal distribution of the wave function among many basis states to a dominance of few basis states (see figs. 1 and 2) leading to an increasing neutron distribution function S_ν in fig. 6. In this context the lower value of the gamma structure function Γ for the $N = 96$ nucleus ^{160}Gd in fig. 8 might at first glance be confusing but one has to realize that Γ also incorporates, beside S_ν and S_π, the wave function fractions f_π

and f_ν. The increasing dominance of the neutron states ($f_\nu \approx 0.75$) and hence the decreasing f_π values lead, despite the large S_ν and S_π values, to a local reduction of Γ. Considering the overall structural evolution it is apparent from our calculations that the Gd and Dy isotopes become less gamma-rigid for high neutron numbers.

All of the Er isotopes have nearly constant values of S_ν and S_π (see fig. 6) which are located at a rather high level comparable to the Gd and Dy isotopes and the wave function is, except for ^{160}Er ($N = 92$), perfectly balanced between neutrons and protons. Therefore, all of the Er isotopes considered show a reduced gamma-rigidity with values for the gamma structure function Γ in fig. 8 even higher than those of the Gd and Dy isotopes. This result is consistent with the trajectory for the Er isotopes in the IBA triangle [4] which lies somewhat above (higher angles) those trajectories for the Gd and Dy isotopes.

4.6 Yb and Hf isotopes

The Yb and Hf isotopes evolve quite differently in the IBA calculations [4], starting out at angles near 40° for $N = 92$ down to angles below 20° for $N \geq 102$. Please note that for ^{170,172}Yb we used the χ-values obtained under the assumption that the second excited 0^+ state in these nuclei is the first excited collective 0^+ state (see ref. [4] for a discussion). At first sight the trend of the two isotopic chains seems to be quite similar. On closer inspection one can, however, observe that the Yb isotopes stay at angles near 30° up to $N = 100$ and θ drops down to 20° for $N = 102$ while θ drops for the Hf isotopes continuously from 30° at $N = 96$ to 10° at $N = 102$, after which an increase in θ is observed to about 17°.

In the present approach the different behavior of the proton distribution function S_π for the Yb and Hf isotopes in fig. 7 is the main reason for the different evolution of Γ for these two isotopic chains, that is visible in fig. 8. While the Yb isotopes start out with a trend towards lower gamma-rigidity (large Γ-values) and drop suddenly to lower Γ-values at $N = 102$, the Hf isotopes start already at significantly lower Γ-values of about 0.3 and drop to even lower values of about 0.15 at $N = 102$. For $N = 104$ the Γ-value increases again slightly only to drop back down for $N = 106$, for which unfortunately no IBA calculations were performed in [4] due to the large boson number.

For Yb the proton distribution function S_π is located at a level of about 0.7 increasing moderately with the neutron number meanwhile for Hf S_π is located at low values of about 0.4. For the Yb isotopes from $N = 92$ to $N = 100$ and for the Hf isotopes from $N = 94$ to $N = 98$ the neutron distribution function S_ν stays nearly at the same level of about 0.77. This would imply a more or less constant behavior (of course at different levels for Yb and Hf) of the gamma structure function Γ for those isotopes. However, in Yb the moderately increasing proton distribution function S_π leads to a reduced gamma-rigidity comparable in its rise with the rise of the Dy isotopes. For Hf isotopes the gamma structure function Γ reveals even a slope down towards increased gamma-rigidity which is caused by the growing inequality in the distribution of the wave function on proton and neutron states. For the Yb isotopes from $N = 102$ to $N = 104$ the high value of the neutron distribution function S_ν suddenly breaks away due to a change from a dominance of neutrons in the 2^+_γ wave function ($f_\nu \approx 0.5$–0.6) to a more dominant proton fraction ($f_\pi \approx 0.6$–0.7) that goes hand in hand with a change from a situation with few neutron quasiparticle states dominating the neutron wave function ($S_\nu \approx 0.77$) to a more equal contribution of many neutron basis states to the neutron wave function ($S_\nu \approx 0.5$) for $N > 100$. Therefore the isotopes go towards a more gamma-rigid structure as the gamma structure function clearly shows. For the Hf isotopes from $N = 100$ to $N = 102$ exactly the same happens to the neutron states with the same intensity as in Yb leading to a further slope down of the gamma-structure function. Finally, for $N = 104$ the Γ-value increases again towards gamma-softness because of a sudden upward peak in S_π characterizing the proton state distribution. Despite the further growth of S_ν for $N = 106$, Γ drops down again. This is due partly to the increasing inequality of the distribution of the wave function among protons and neutrons and partly due to the return of S_π to its usual value for this isotopic chain.

4.7 Empirical relation between Γ and θ

The discussion above shows that it is possible to relate the evolution of Γ, which is based on the underlying dominant two-quasiparticle configurations in the 2^+_γ state, to the trends observed in the IBA parameters of ref. [4].

However, the situation is not quite as simple, as can be observed by shifting our attention to the energy ratio

$$R_{22} \equiv \frac{E(2^+_\gamma)}{E(2^+_1)}\,.$$

It is well known that gamma-soft nuclei near the $O(6)$ limit exhibit R_{22}-values near 2.5, while in the well-deformed nuclei under investigation here, R_{22} will take on much larger values.

Figure 9 shows the calculated values of K from eq. (11) against the R_{22}-values for the nuclei under consideration. For this we used the IBA parameters from ref. [4] as well as our own IBA fits in the ECQF for the Sm nuclei. It is obvious that there is a direct correlation between the stiffness of the potential in the gamma-direction and the energy of the gamma-vibration relative to the energy of the first excited 2^+ state which sets the energy scale in the nucleus.

At the same time, the R_{22}-values do not correlate uniquely with the Γ-values (see fig. 10) or the IBA parameter χ (not shown). This means that neither θ nor Γ can be used alone to describe the gamma-stiffness. In particular, one has to note that the same value for R_{22} (same K) can be obtained for very different values of Γ. While this is not completely surprising, since K depends

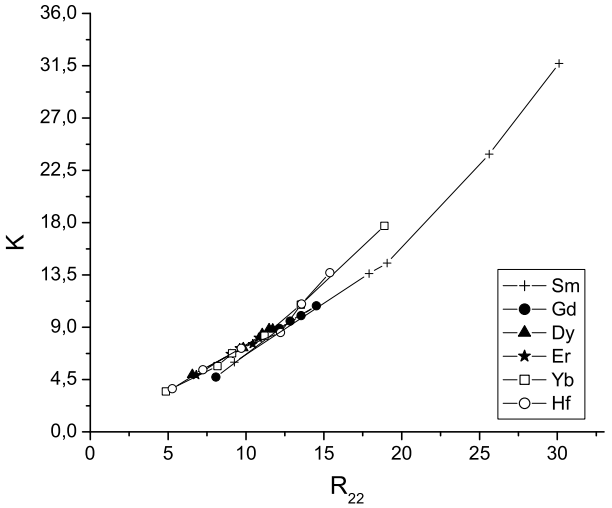

Fig. 9. The stiffness K of the potential $V(\beta,\gamma) \equiv \langle H \rangle$ in the γ-direction at its minimum value (see eq. (11)) as a function of R_{22} for the nuclei under consideration. Both values are calculated using the IBA parameters from ref. [4], except for Sm, for which parameters were determined in this work.

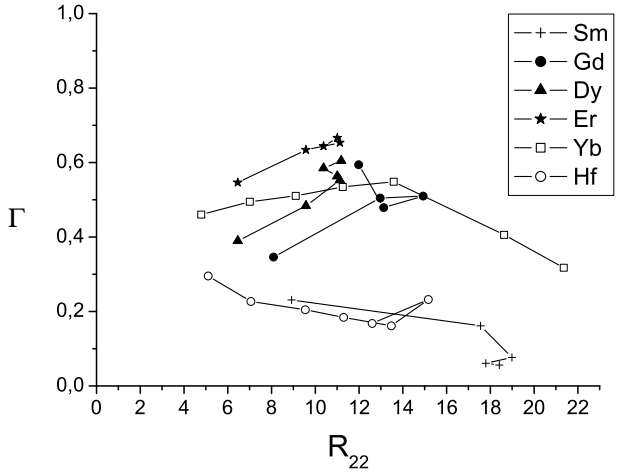

Fig. 10. Values of the gamma structure function Γ *vs.* the experimental energy ratio $R_{22} \equiv \frac{E(2^+_\gamma)}{E(2^+_1)}$.

on χ, ζ, N_B, and β_{min}, it also points to a more complicated relation between Γ and θ.

While there seems to be no physically intuitive or obvious relation between Γ and the angles θ_{IBA}, as defined in eq. (7), we have empirically found that a simple linear combination of R_{22} and Γ allows us to reasonably reproduce θ_{IBA}.

For an isotope with N neutrons and Z protons we define the angle

$$\tilde{\theta}(Z,N) = \Gamma(Z,N) + \frac{2.5}{R_{22}(Z,N)}\,, \qquad (13)$$

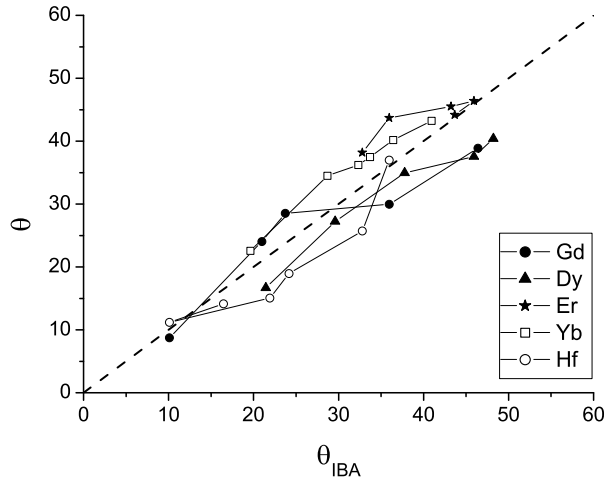

Fig. 11. Angles θ calculated using eq. (14) against the angles obtained by the IBA fits [4].

which will however be non-zero also for the Sm isotopes, which should lie directly on the $U(5)$ to $SU(3)$ leg of the symmetry triangle and thus have $\theta_{IBA} = 0$.

Therefore, we subtract the $\tilde{\theta}$-value for the Sm isotope with the same neutron number from the value for a given nucleus with proton number Z and neutron number N:

$$\theta = \tilde{\theta}(Z,N) - \tilde{\theta}(62,N). \qquad (14)$$

Due to missing experimental data for Sm nuclei with $N > 98$, no calculations in the framework of our model could be performed for these isotopes. Therefore, we have used the Γ-value for the $N = 98$ isotope ^{160}Sm for all Sm isotopes with $N > 98$.

Figure 11 shows the resulting angles θ from eq. (14) against the angles θ_{IBA} obtained from the IBA fits [4] showing a clear correlation between both values. It is unfortunately not clear what the physical meaning of this correlation is.

4.8 Summary and conclusions

In summary, we have shown a connection between the structural evolution of well-deformed even-even rare-earth nuclei within the IBA symmetry triangle and the two-quasiparticle content of the gamma-vibration in these nuclei. The evolution of the two-quasiparticle content of the gamma-vibration was determined on the basis of a simplified RPA approach using two-quasiparticle states based on Nilsson wave functions and including the partial occupation near the Fermi energy due to pairing. The evolution within the IBA symmetry triangle can be related to a function Γ (gamma structure function) that is large if the gamma-vibration is dominated by a few equally important two-quasiparticle orbitals for protons *and* neutrons. Γ is small if there is a significant imbalance between proton and neutron components in the wave function or if the wave function for protons and neutrons contains only smaller contributions from many two-quasiparticle states.

It was also possible to roughly reproduce the angle θ in the IBA symmetry triangle for a large number of well-deformed even-even rare-earth nuclei using a single parameter free expression including Γ and the energy ratio $R_{22} = E(2^+_\gamma)/E(2^+_1)$. While the theoretical basis of this simple expression remains unclear, it certainly shows that the IBA parameters used to describe the structural evolution can be related to the underlying single-particle structure within the Nilsson model.

Useful discussions with P. von Brentano, A. Dewald, E.A. McCutchan, and F. Iachello are gratefully acknowledged. This work was supported in part by the U.S. DOE under Grant No. DE-FG02-91ER-40609.

References

1. S.G. Nilsson, Mat.-Fys. Medd. K. Dan. Vidensk. Selsk. **29**, No. 16 (1955).
2. A. Arima, F. Iachello, Phys. Rev. Lett. **35**, 1069 (1975).
3. P.O. Lipas, P. Toivonen, D.D. Warner, Phys. Lett. B **155**, 295 (1985).
4. E.A. McCutchan, N.V. Zamfir, R.F. Casten, Phys. Rev. C **69**, 064306 (2004).
5. R.F. Casten, D.D. Warner, in *Progress in Particle and Nuclear Physics*, edited by D. Wilkinson, Vol. **9** (Pergamon, Oxford, 1983) p. 311.
6. E.A. McCutchan, N.V. Zamfir, Phys. Rev. C **71**, 054306 (2005).
7. E.A. McCutchan, R.F. Casten, N.V. Zamfir, Phys. Rev. C **71**, 061301(R) (2005).
8. D.R. Bès, P. Federman, E. Maqueda, A. Zuker, Nucl. Phys. **65**, 1 (1965).
9. V.G. Soloviev, Sov. J. Part. Nucl. **9**, 343 (1978).
10. V.G. Soloviev, *Theory of the Nucleus. Quasiparticles and Phonons* (Institute of Physics, Bristol, England, 1992) (Russian original, Energoatomizdat, Moscow, 1989).
11. V.G. Soloviev, A.V. Sushkov, N.Yu. Shirikova, Phys. Part. Nucl. **25**, 157 (1994).
12. V.G. Soloviev, A.V. Sushkov, N.Yu. Shirikova, Phys. Part. Nucl. **27**, 667 (1996).
13. D.G. Burke, V.G. Soloviev, A.V. Sushkov, N.Yu. Shirikova, Nucl. Phys. A **656**, 287 (1999).
14. P. Ring, P. Schuck, in *The Nuclear Many Body Problem* (Springer, Heidelberg, 1980) pp. 200.
15. A.J. Rassey, Phys. Rev. **109**, 949 (1958).
16. S. Raman, C.W. Nestor jr., P. Tikkanen, At. Data Nucl. Data Tables **78**, 1 (2001).
17. Nucl. Data Sheets, through Vol. **94**, Issue 4 (2001).
18. T.R. Werner, J. Dudek, At. Data Nucl. Data Tables **50**, 179 (1992).
19. S. Nilsson, I. Ragnarsson, in *Shapes and Shells in Nuclear Structure* (Cambridge Universits Press, Cambridge, 1995) p. 126.
20. E.S. Hernández, A. Plastino, Phys. Rev. C **5**, 1888 (1972).
21. J.N. Ginocchio, M.W. Kirson, Nucl. Phys. A **350**, 31 (1980).
22. J.N. Ginocchio, in *Interacting Bose-Fermi Systems in Nuclei*, edited by F. Iachello (Plenum, New York, 1980) p. 179; A.E.L. Dieperink, O. Scholten, in *Interacting Bose-Fermi Systems in Nuclei*, edited by F. Iachello (Plenum, New York, 1980) p. 167; J.Q. Chen, P. Van Isacker, in *Interacting Bose-Fermi Systems in Nuclei*, edited by F. Iachello (Plenum, New York, 1980) p. 193; R. Gilmore, D.H. Feng, in *Interacting Bose-Fermi Systems in Nuclei*, edited by F. Iachello (Plenum, New York, 1980) p. 149.
23. K. Heyde, in *Algebraic Approaches to Nuclear Structure*, edited by R.F. Casten (Harwood Academic Publishers, 1993) p. 376.
24. G. Gneuss, U. Mosel, W. Greiner, Phys. Lett. B **30**, 397 (1969).
25. G. Gneuss, U. Mosel, W. Greiner, Phys. Lett. B **31**, 269 (1970).
26. G. Gneuss, W. Greiner, Nucl. Phys. A **171**, 449 (1971).
27. Jing ye Zhang, R.F. Casten, N.V. Zamfir, Phys. Lett. B **407**, 201 (1997).
28. D. Troltenier, J.A. Maruhn, W. Greiner, Z. Phys. A **348**, 1 (1994).
29. J.A. Cizewski, R.F. Casten, G.J. Smith, M.L. Stelts, W.R. Kane, H.G. Börner, W.F. Davidson, Phys. Rev. Lett. **40**, 167 (1978).
30. O. Scholten, F. Iachello, A. Arima, Ann. Phys. (N.Y.) **115** 325 (1978).